View metadata, citation and similar papers at core.ac.uk
brought to you by CORE
provided by RERO DOC Digital Library

Int J Cardiovasc Imaging (2013) 29:1565–1574
DOI 10.1007/s10554-013-0228-4

ORIGINAL PAPER

Image quality of low-dose CCTA in obese patients: impact of high-definition computed tomography and adaptive statistical iterative reconstruction

Cathérine Gebhard · Tobias A. Fuchs · Michael Fiechter · Julia Stehli · Barbara E. Stähli · Oliver Gaemperli · Philipp A. Kaufmann

Received: 21 January 2013 / Accepted: 19 April 2013 / Published online: 28 April 2013
© Springer Science+Business Media Dordrecht 2013

Abstract The accuracy of coronary computed tomography angiography (CCTA) in obese persons is compromised by increased image noise. We investigated CCTA image quality acquired on a high-definition 64-slice CT scanner using modern adaptive statistical iterative reconstruction (ASIR). Seventy overweight and obese patients (24 males; mean age 57 years, mean body mass index 33 kg/m^2) were studied with clinically-indicated contrast enhanced CCTA. Thirty-five patients underwent a standard definition protocol with filtered backprojection reconstruction (SD-FBP) while 35 patients matched for gender, age, body mass index and coronary artery calcifications underwent a novel high definition protocol with ASIR (HD-ASIR). Segment by segment image quality was assessed using a four-point scale (1 = excellent, 2 = good, 3 = moderate, 4 = non-diagnostic) and revealed better scores for HD-ASIR compared to SD-FBP (1.5 ± 0.43 vs. 1.8 ± 0.48; $p < 0.05$). The smallest detectable vessel diameter was also improved, 1.0 ± 0.5 mm for HD-ASIR as compared to 1.4 ± 0.4 mm for SD-FBP ($p < 0.001$). Average vessel attenuation was higher for HD-ASIR (388.3 ± 109.6 versus 350.6 ± 90.3 Hounsfield Units, HU; $p < 0.05$), while image noise, signal-to-noise ratio and contrast-to noise ratio did not differ significantly between reconstruction protocols (p = NS). The estimated effective radiation doses were similar, 2.3 ± 0.1 and 2.5 ± 0.1 mSv (HD-ASIR vs. SD-ASIR respectively). Compared to a standard definition backprojection protocol (SD-FBP), a newer high definition scan protocol in combination with ASIR (HD-ASIR) incrementally improved image quality and visualization of distal coronary artery segments in overweight and obese individuals, without increasing image noise and radiation dose.

Keywords Cardiac computed tomography · Adaptive statistical iterative reconstruction · Obesity

Introduction

Obesity has been related to numerous risk factors such as hypertension, hypercholesterolemia and diabetes and is associated with higher rates of mortality, resulting from coronary artery disease (CAD) [1]. Most imaging techniques face difficulties when dealing with this subset of patients and anatomical imaging techniques including coronary computed tomography angiography (CCTA) are no exception; in fact, despite the generally high diagnostic performance of CCTA for the assessment of CAD, a decline in image quality due to an increase in X-ray scatter and image noise is noted when using standard protocols in obese patients [2, 3]. The higher image noise causes particularly poor delineation of smaller, distal vessels as well as non-calcified atherosclerotic lesions [4]. Recently, a high-definition CT (HDCT) scanner with improved in-plane spatial resolution of 230 μm has been introduced. As improved spatial resolution goes along with a decrease in signal-to-noise ratio due to increased noise, this technical refinement has been complemented by a novel statistical

Cathérine Gebhard and Tobias A. Fuchs contributed equally to this work.

C. Gebhard · T. A. Fuchs · M. Fiechter · J. Stehli · B. E. Stähli · O. Gaemperli · P. A. Kaufmann (✉)
Department of Radiology, Cardiac Imaging, University Hospital Zurich, Ramistrasse 100, NUK C 42, 8091 Zurich, Switzerland
e-mail: pak@usz.ch

P. A. Kaufmann
Zurich Center for Integrative Human Physiology (ZIHP), University of Zurich, Zurich, Switzerland

iterative reconstruction (ASIR) algorithm for noise reduction. Unlike the standard filtered back projection technique (FBP), iterative reconstruction entails fewer assumptions regarding noise distribution within an image and operates with an iterative process of mathematic and statistical modelling to identify and selectively reduce noise [5, 6] within the reconstructed images while maintaining spatial resolution and image quality [7–9]. Latest studies have shown that the use of ASIR in low dose HDCT was associated with higher resolution than standard definition CT (SDCT) but maintained image quality and equally low radiation dose in a normal weight population [10]. Although this new reconstruction technique has been shown to improve image quality in abdominal CT in large body size adults [11], no data are available supporting the use of ASIR in combination with HDCT in an overweight and obese population.

Therefore, we hypothesized that HD acquisition with ASIR reconstruction yields superior image quality in CCTA of overweight and obese patients compared to a conventional standard definition (SD) acquisition and standard (filtered backprojection, FBP) reconstruction technique using the same 64-slice HDCT scanner for both protocols.

Materials and methods

Patients

We included 70 overweight and obese patients (24 males; mean age 57 years, mean body mass index 33 kg/m^2) with clinically indicated contrast enhanced CT of which 35 underwent a novel HD acquisition protocol with ASIR. Each case was matched by gender, age, body mass index and coronary artery calcifications with one control that underwent a SD protocol with FBP reconstruction. Patients were eligible for the study if the BMI was >28 kg/m^2. The need to obtain written informed consent in this study was waived by the institutional review board (local ethics committee) since, according to Swiss law on clinical investigations, informed consent is not required if the nature of the study is purely retrospective. Indications for CCTA were typical ($n = 15$) or atypical angina ($n = 17$), dyspnea ($n = 12$), previous positive stress imaging study ($n = 7$), preoperative risk evaluation for non-cardiac surgery ($n = 4$), impaired left ventricular function ($n = 4$), and other reasons (including risk profile and arrhythmias) for suspected CAD ($n = 11$). Exclusion criteria for CCTA examination were renal failure (glomerular filtration rate <30 ml/min), known allergy to iodine contrast material, severe claustrophobia, pregnancy, and high heart rate in the presence of contraindications to beta-blockade.

Coronary CT acquisition

All scans were performed on a 64-HDCT scanner (Discovery HD 750, GE Healthcare) with prospective electrocardiogram (ECG)-triggering, a BSA-adapted contrast media bolus (Visipaque 320 mg/ml, GE-Healthcare) with a contrast volume of 40–105 ml and a flow rate between 3.5 and 5.0 ml/s corresponding to an iodine delivery rate ranging from 1.1 to 1.6 g/s [12–14] and iv β-blockers, if needed, to achieve a heart rate lower than 65 beats/min and 0.4 mg sublingual nitro-glycerine were administered to all patients immediately before the study. The first 35 patients were examined with our SD protocol [12] and images were reconstructed with FBP. After introducing HD scanning with ASIR reconstruction at our department, CCTA of the first 35 consecutive patients were acquired in HD, which was 230 μm, and images were reconstructed with high-resolution and a blending of 30 % ASIR into FBP. Radiation dose was calculated from the dose-length product using a conversion factor of 0.014 mSv/(mGy x cm) [15]. The scanning parameters included 64 × 0.625 mm collimation, a rotation time of 0.35 s, and BMI adjusted tube voltage (100–120 kV) and current (450–700 mA) .

CCTA analysis

On a dedicated workstation (Advantage AW 4.4, GE Healthcare) where mean signal value and SD (noise) in

Table 1 Patient baseline and CT acquisition characteristics

	FBP SDCT protocol $n = 35$	ASIR HDCT protocol $n = 35$
Male sex, no. of patients (of total)	24 (35)	34 (35)
Age (years)	58 ± 2	56 ± 4
BMI (kg/m^2)	33.8 ± 1	32.9 ± 1
Calcifications (number of segments)	61	63
mSv	2.5 ± 0.1	2.3 ± 0.1
DLP (mGy × cm)	176.0 ± 7.0	163.3 ± 10.5
$CTDI_{VOL}$ (mGy)	17.4 ± 0.7	16.0 ± 0.9
Heart rate (bpm)	59.5 ± 1.2	59.5 ± 1.2
Tube voltage (kV)	116 ± 1.4	112 ± 1.7
Tube current (mA)	645.7 ± 4.8	632.9 ± 5.0
Contrast flow (ml/s)	4.8 ± 0.1	4.9 ± 0.1
Contrast volume (ml)	84.3 ± 2.6	82.3 ± 1.8
Number of stents	4	5
Coronary artery disease (number of patients)	14	13
Betablcoker (mg)	7.5 ± 1.4	10.6 ± 1.5

Values are given as mean ± standard deviation (SD) if appropriate

FBP filtered back projection, *SD* standard definition, *ASIR* adaptive iterative reconstruction algorithm, *HDCT* high definition computed tomography

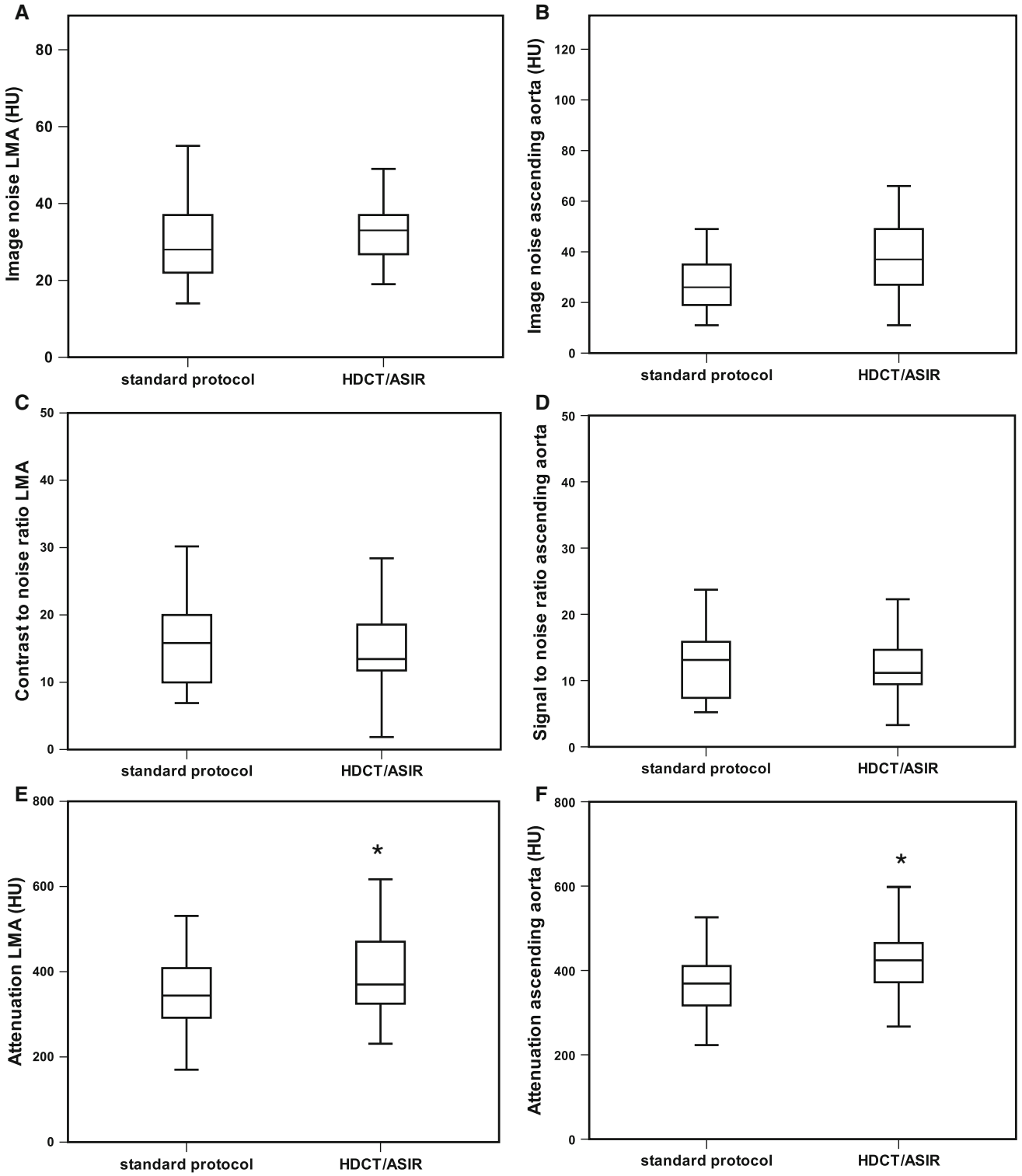

Fig. 1 *Boxplots* of objective measurements of both protocols. **a** Image noise LMA (left main coronary artery). **b** Image noise ascending aorta. **c** Contrast-to-noise ratio in vessel lumen of the left main coronary artery (LMA) **d** Signal-to-noise ratio in the ascending aorta. **e** Attenuation (HU) in the left main coronary artery. **f** Attenuation (HU) in the ascending aorta. Data are presented as mean ± SD. $*p < 0.05$

Hounsfield units (HU) were measured, a region of interest (ROI) was placed in the aortic root (0.5 cm^2) and in the proximal left main artery (LMA) (5 mm^2). The vessel contrast was measured as the difference in mean attenuation in HU in the contrast enhanced vessel lumen and the mean attenuation in HU in the adjacent perivascular tissue. The results were

Table 2 Image quality parameters

	FBP SD protocol	ASIR HDCT protocol
Attenuation (HU, LMA), mean ± SD	350.6 ± 90.3	388.3 ± 109.6*
Attenuation (HU, aorta), mean ± SD	370.9 ± 77.9	430.51 ± 88.9*
SNR (LMA), mean ± SD	12.2 ± 5.7	13.1 ± 7.7
SNR (aorta), mean ± SD	15 ± 1.3	12.7 ± 5.8
CNR, mean ± SD	15.8 ± 6.9	15.6 ± 8.9
Image quality, mean ± SD	1.8 ± 0.48	1.5 ± 0.43*
Quality score 1 (number of segments)	149	282
Quality score 2 (number of segments)	221	128
Quality score 3 (number of segments)	59	45
Quality score 4 (number of segments)	35	22
Total number of segments analyzed (*n*)	464	477
Minimal visible vessel diameter (mm), mean ± SD	1.3 ± 0.2	1.0 ± 0.3*
Minimal visible vessel area (mm^2), mean ± SD	1.4 ± 0.4	1.0 ± 0.5*
Percentage of diagnostic segments, mean ± SD	93 ± 14.5	95 ± 10.9

Values are presented as indicated

* $p < 0.05$

used to calculate contrast to noise ratio (CNR). To standardize the analysis, images were displayed with a fixed window level at 240 HU and a window width at 1,200 HU.

Image quality analysis

Qualitative image analysis was performed by two independent blinded and experienced coronary CCTA readers. The original transaxial slices were visually examined, assisted by oblique and curved multiplanar reconstructions. Each coronary artery segment was classified using a 4-point score: (1) excellent; (2) good, minor artifacts; (3) fair, moderate artifacts but still diagnostic and [4] nondiagnostic (Fig. 6). For each coronary artery segment classified as not excellent (i.e., scores: 2–4) the observers noted the causes of image quality impairment as motion artifacts, image noise, insufficient contrast opacification, or high contrast artifacts. For any disagreement in data evaluation between the two readers, consensus agreement was achieved. Finally, all CCTA studies were reviewed for the presence or absence of significant coronary artery stenosis defined as luminal narrowing exceeding 50 % in diameter. Coronary artery segments with a diameter of <1.5 mm can only be visualized if clear delineation of the vessel walls, low image noise, and excellent attenuation of the vessel lumen is provided. Thus, diameter and area of smallest visible distal segments (segments number 4, 8, 9, 10, 12, 14, 15, 16) were used as an parameter to analyse image quality (Fig. 7). Diameter measurements were performed with an electronic caliper tool (Volume Viewer, GE Healthcare, Milwaukee, USA).

Statistical analysis

Quantitative variables were expressed as mean ± SD and categorical variables as frequencies or percentages. Comparisons of image noise, signal to noise ratio and CNR between the two groups were performed using student's *t* test for continuous variables with normal distributions and the Mann–Whitney *U* test for continuous variables with non-normal distributions. Mixed model analysis of variance was used to compare both scan algorithms with respect to image quality scores and to assess differences across the four main arteries (left main, right coronary artery, left anterior descending, and left circumflex) in terms of these scores. Spearman's rank correlation coefficient was used to assess the relationship between BMI, image quality, radiation dose and contrast volume. The generalized estimating equations analysis was used to compare scan algorithms in terms of the percentage of times segments were rated as having diagnostic IQ. Correlation coefficients were calculated to compare BMI with the mean image quality scores of all coronary segments on a per patient basis. The correlation structure imparted by the inclusion of data from multiple segments per patient was modelled by assuming data to be correlated when acquired from the same patient. All analyses were performed with statistics software (SPSS version 20.0 for Microsoft Windows). A two-tailed *p* value of <0.05 was deemed significant.

Results

Study population

The study population consisted of 70 patients, including 22 women, with a mean age of 57 ± 19 years, and a mean BMI of 33 ± 5.7 kg/m^2. The average BMI in group A (standard protocol) was 33.8 ± 1 kg/m^2 (range 29–58 kg/m^2) and 32.9 ± 1 in group B (ASIR protocol) (range

28–61 kg/m^2). 28 % (20/70) of patients were overweight (BMI 28–30 kg/m^2), 46 % (30/70) patients were obese (BMI 30–35 kg/m^2) and 26 % (20/70) of patients were morbidly obese (BMI > 35, range 35–61 kg/m^2). The patient baseline characteristics are listed in Table 1. A total contrast amount of 83.2 ± 13 ml at an injection rate of 4.9 ± 0.5 ml/s was administered (Table 1). Patients were adequately matched for gender, age, body mass index and coronary artery calcifications (p = NS).

Radiation dose

The mean tube current and mean tube voltage was 645.7 ± 4.8 mA and 116 ± 1.4 kV for protocol A and 632.9 ± 5.0 mA and 112 ± 1.7 kV for protocol B. (Table 1). The average dose-length product (DLP) was 176.0 ± 7.0 (mGy x cm) in protocol A and 163.3 ± 10.5 (mGy x cm) in protocol B. resulting in an average effective radiation dose of 2.5 ± 0.1 mSv (range 1.4–4.3 mSv) and

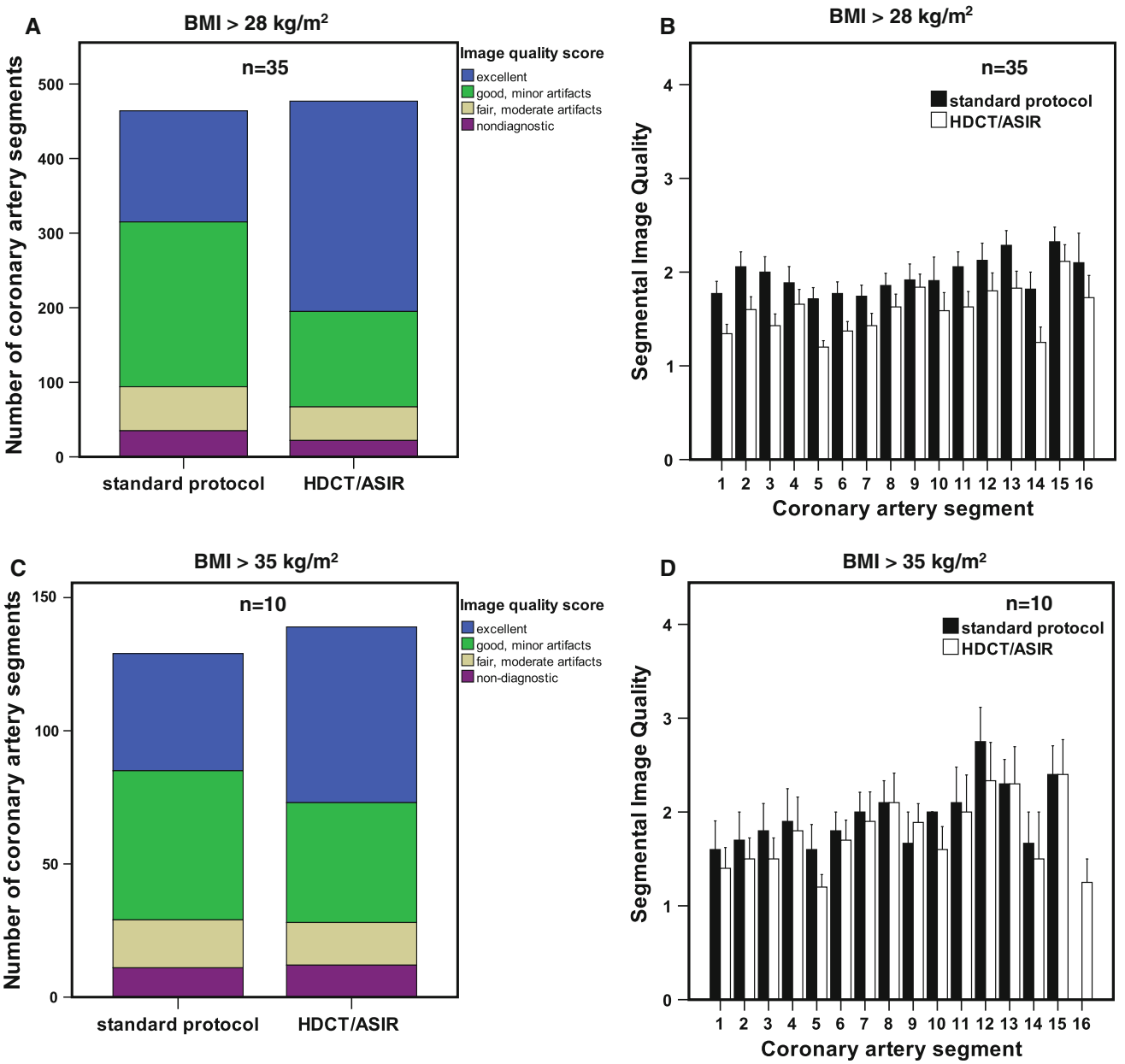

Fig. 2 **a** Image quality score groups for all evaluated coronary segments in all study subjects. **b** Image score (mean ± SD) for each segment in all study subjects. **c** Image quality score groups for all evaluated coronary segments in patients with BMI > 35 kg/m^2. **d** Image score (mean ± SD) for each segment in patients with BMI > 35 kg/m^2. *HDCT* high definition computed tomography, *ASIR* adaptive iterative reconstruction

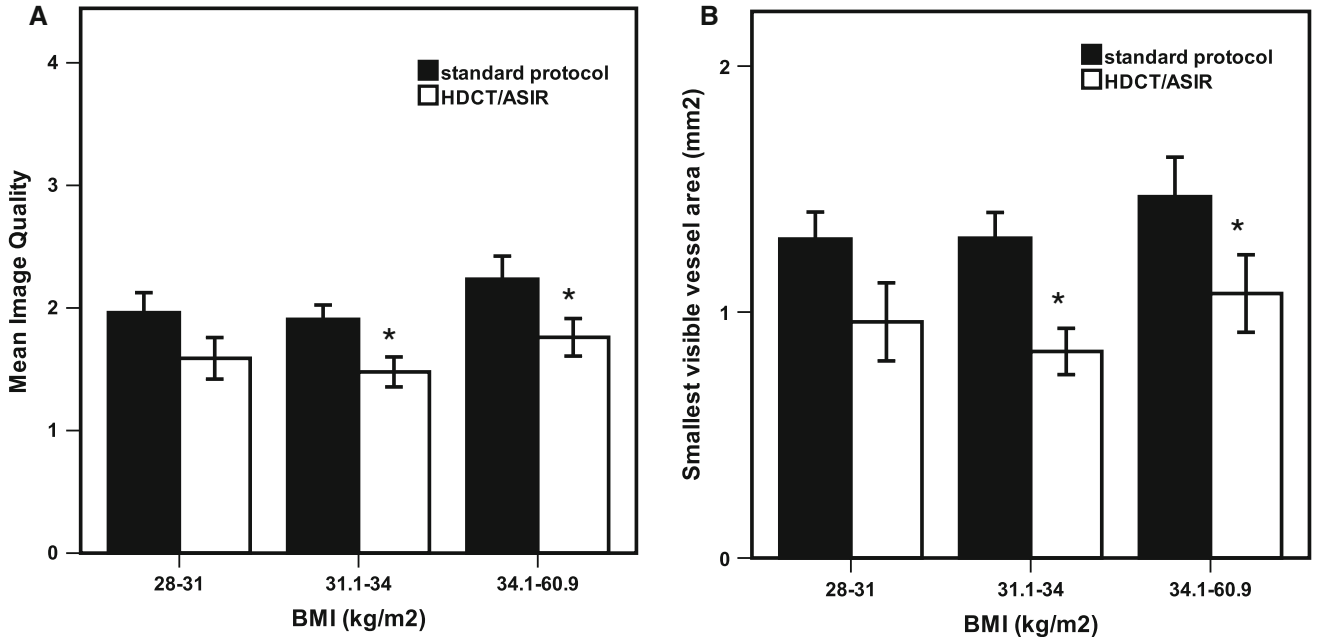

Fig. 3 **a** Tertile analysis according to BMI of mean per patient image quality score (mean ± SEM) in both groups. **b** Tertile analysis according to BMI of minimal area of coronary artery segments that could be visualized in both groups (mean ± SEM). *HDCT* high definition computed tomography. *ASIR* adaptive iterative reconstruction. Data are presented as mean ± SEM. *$p < 0.05$

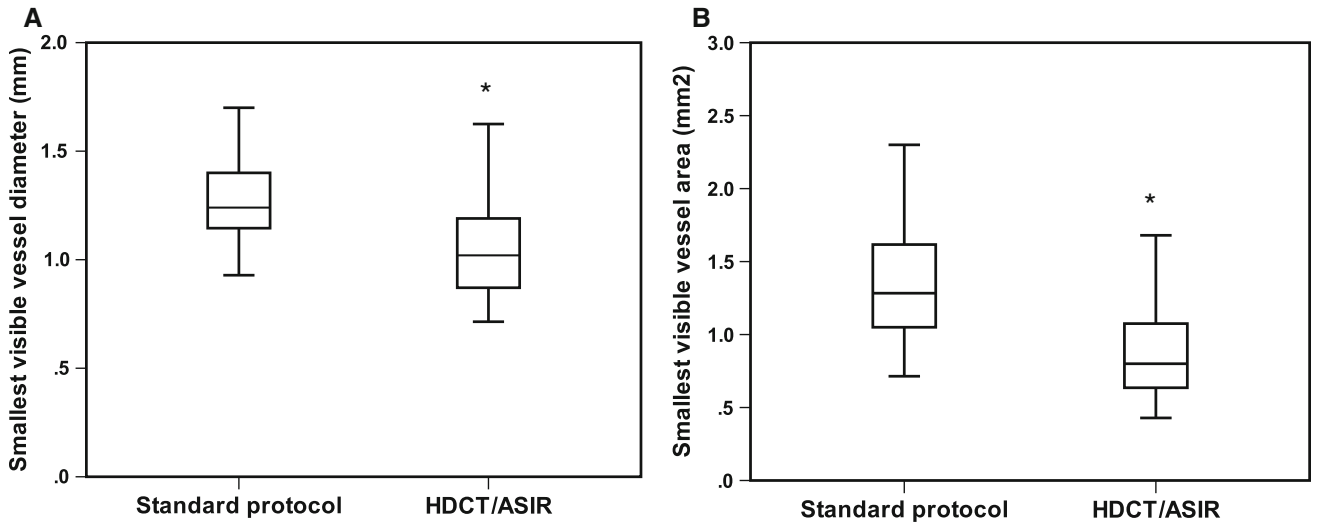

Fig. 4 Minimal diameter (**a**) and area (**b**) of smallest coronary artery segments that could be visualized in both groups. Data are presented as mean ± SD. *$p < 0.05$

2.3 ± 0.1 mSv (range 1.1–5.4 mSv; p = NS), respectively (Table 1).

Image noise

Image noise measured in the ascending aorta and the left main coronary artery (LMA) was similar in both groups (p = NS, Fig. 1a, b). Attenuation (HU) in the ascending aorta and the LMA was significantly increased in group B compared to groups A ($p = 0.041$, Fig. 1e, f). There was no significant difference in signal to noise ratio (SNR) and CNR with protocol A compared to the standard protocol B (p = NS, Fig. 1c, d; Table 2).

Image quality

A total of 941 coronary artery segments were evaluated. The total number of segments is not equal due to anatomic variations with not all segments being present in all patients. After consensus agreement, image quality was rated as

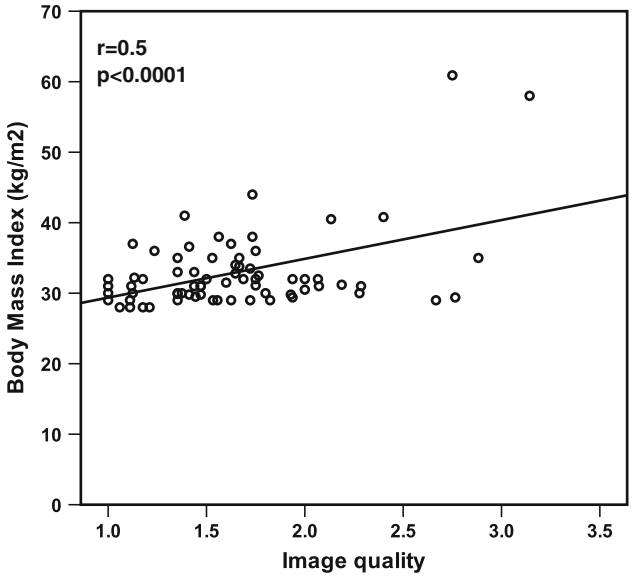

Fig. 5 Correlation coefficient between image quality and BMI (body mass index) for entire study cohort (Spearman's correlation $r = 0.5$, $p < 0.0001$)

excellent in 32 % of coronary segments (149/464), good in 47 % (221/464), fair in 13 % (59/464) and non-diagnostic in 7 % (35/464) in group A while image quality was rated as excellent in 59 % of coronary segments (282/477), good in 26 % (128/477), fair in 9 % (45/477) and non-diagnostic in 5 % (22/477; Chi square test $p = 0.06$ versus group A) in group B (Fig. 2a, b; Table 2). Mean scores of subjective image quality were significantly better when using protocol B (1.5 ± 0.43) as compared with protocol A (1.8 ± 0.48; $p = 0.02$) (Table 2) and improvement of image quality scores was distributed over all coronary segments (Fig. 2b). Mean image quality scores were non-diagnostic (Likert score >3) in three patients in group A and one patient in group B. A subgroup analysis in patients with BMI > 35 kg/m^2 revealed a slightly lower, but not significant, overall image quality compared to the entire patient cohort (1.8 ± 0.5 in patients with BMI > 35 kg/m^2 versus 1.6 ± 0.6 in total cohort, $p = 0.1$). When image quality was compared between protocol A and protocol B in these morbidly obese patients, mean scores of image quality were significantly higher when using protocol B compared to protocol A (2.3 ± 0.8 versus 1.8 ± 0.5, $p = 0.036$, Fig. 2c, d). When the study population was divided into tertiles, according to BMI, the largest increase in image quality (=lowest Likert quality score) and visibility of small vessels with ASIR/HDCT was detected in the middle tertile BMI group (31.1–34 kg/m^2) ($p < 0.002$ vs. standard protocol for image quality and $p < 0.003$ vs. standard protocol for smallest visible vessel area, Fig. 3a, b). In the lowest tertile group image quality and smallest visible vessel area improved with ASIR, however, this difference did not reach statistical significance. In the highest tertile group (BMI 34.1–60.9 kg/m^2), a significant improvement of image quality as well as smallest visible vessel area was seen ($p < 0.05$ vs. standard protocol). However, these differences were less compared to the middle tertile group (Fig. 3a, b). There were 4 stented segments noted in group A and 5 in group B (Table 1), all classified as patent with diagnostic image quality. Fourteen patients in group A and 13 patients in group B were diagnosed with some degree of CAD (Table 1). Minimal diameter and area of coronary artery segments that could be visualized with clear delineation of the vessel walls and sufficient attenuation of the vessel lumen were significantly smaller in protocol B compared to standard protocol A ($p < 0.0001$, Fig. 4a, b; Table 2). Mean diameter was 1.3 ± 0.2 mm in group A and 1.0 ± 0.3 mm in group B. Accordingly, mean area was 1.4 ± 0.4 mm^2 in group A and 1.0 ± 0.5 mm^2 in group B ($p < 0.001$; Fig. 4a, b; Table 2). Patients with higher BMI received more contrast ($r = 0.5$; $p < 0.001$) and had significantly increased effective radiation dose exposure ($r = 0.68$; $p < 0.0001$) compared to patients with lower BMI. Overall, there was a modest but significant correlation between BMI and impaired image quality ($r = 0.5$; $p < 0.0001$; Fig. 5) in the entire study group, suggesting that with increasing BMI, there was decreasing image quality noted with both types of scans (Figs. 6, 7).

Discussion

The prevalence of obesity steadily increases in the general population, thereby raising the rate of challenging patients for diagnostic imaging. However, CCTA in obese patients has several limitations with regard to image quality [16] and thus, is associated with reduced sensitivity and specificity when compared to invasive angiography [17]. This study shows that using a protocol that includes HD acquisition and ASIR, improves image quality and vessel visualization of CCTA in patients with a BMI > 28 kg/m^2 compared to standard protocol. Our findings support prior results suggesting improved CCTA quality by using ASIR and extends the potential of increased diagnostic CCTA to an obese population.

A limitation of CCTA in clinical practice is exposure to ionizing radiation. The use of reduced tube voltage has been shown to significantly reduce effective radiation dose but is difficult to apply in obese patients since image quality in these patients is usually adversely affected by beam hardening and photon scatter and must be weighed against the increase in image noise [2, 3]. Accordingly, previous CCTA studies have reported high radiation doses in overweight and obese populations in the range of 15.6–22 mSv [4, 18]. Since patients with a BMI > 30 kg/m^2 have only poorly

been represented in other studies [19–22], we included patients with a BMI ranging between 28 and 61 kg/m^2. Despite including larger patients, mean effective radiation dose in the present study was as low as 2.4 mSv.

One of the main reasons that CCTA has become widely accepted in clinical routine is its robustness for imaging coronary arteries. Therefore, the lowest achievable rate of non-diagnostic coronary artery segments is crucial for the diagnostic performance of CTCA. Indeed, the number of non-diagnostic segments was notably low in obese patients who underwent scanning by applying the new protocol. Moreover, image quality and visualization of distal coronary artery segments were substantially improved. Further, although higher iodine concentrations are frequently recommended for obese patients, it is notable that 95 % of segments in our patient cohort were successfully imaged with a mean iodine contrast volume of 83 ml at a mean intravenous flow rate of 5 ml/s.

Our study is the first to document that the use of high-definition acquisition results in a better visualization of vessel wall and vessel attenuation. Accordingly, we detected improvements in image quality of distal coronary artery segments that could be visualized at a diameter as small as 0.7 mm. However, higher image resolution is usually achieved at the cost of an increase in image noise. The use of image reconstruction with ASIR in combination

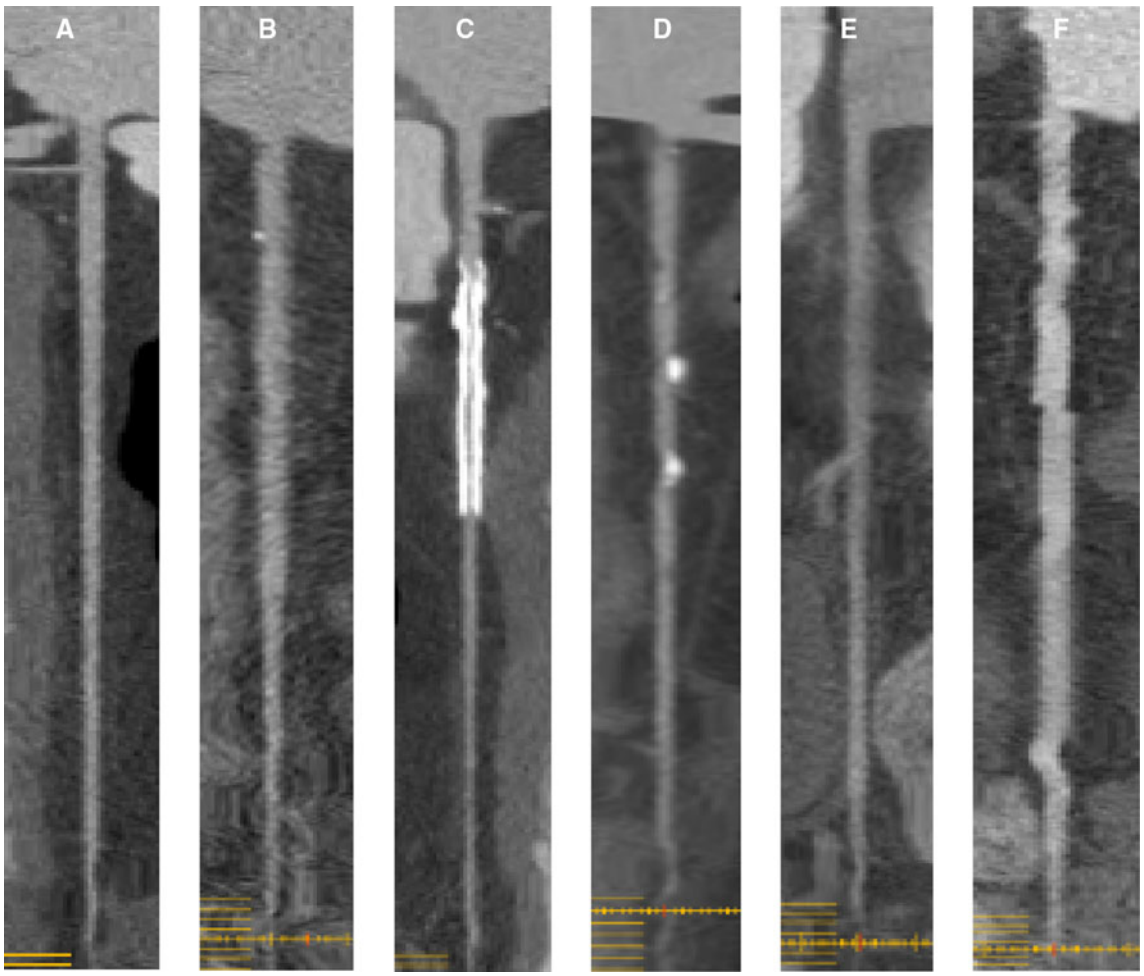

Fig. 6 Representative images demonstrating examples of artefact types deteriorating image quality and the different image quality scores. Images were graded as follows: 1 = Excellent: complete absence of motion artifacts, excellent SNR, and clear delineation of vessel walls are present with the ability to assess luminal stenosis as well as plaque characteristics. 2 = Good: non-limiting motion artifacts, reduced SNR, or calcifications are present, with preserved ability to assess luminal stenosis as well as plaque characteristics. 3 = Adequate: reduced image quality because of any combination of noise, motion, poor contrast enhancement, or calcium that significantly impairs ease of interpretation. Image quality is sufficient to rule out significant stenosis. 4 = Nondiagnostic: reduced image quality that precludes adequate assessment of stenosis. **a** No artefacts and clear delineation of vessel wall (image quality score 1). **b** Beam hardening artefact and motion artefact of the right coronary artery (image quality score 4). **c** Moderate partial volume artefact from the highly attenuated metal stent strut (image quality score 2). **d** Minor artefact due to coronary vessel wall calcification, minor motion artefact (image quality score 2). **e** Insufficient contrast opacification and motion artefact (image score 4). **f** Step artefact and excessive image noise (image quality score 4)

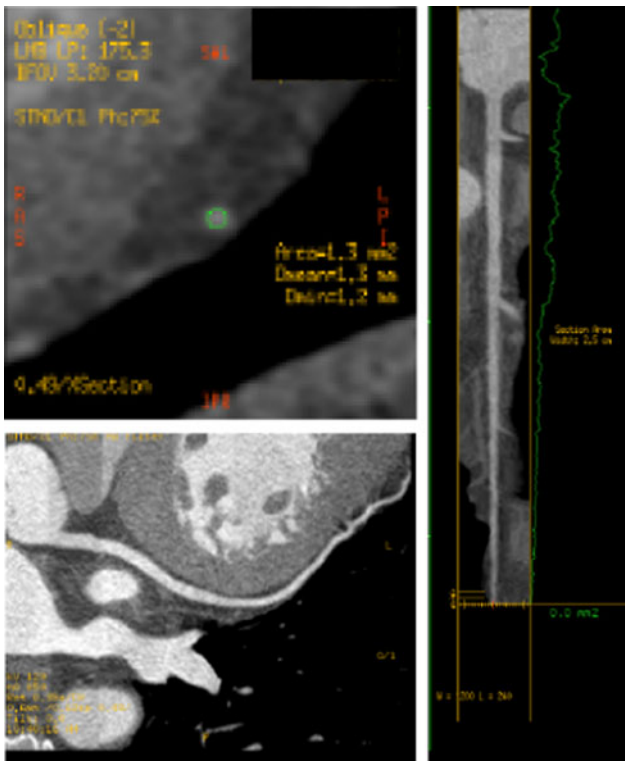

Fig. 7 Representative example of diameter and area measurement in the distal segment [15] of the left circumflex artery

with a high-definition acquisition protocol resulted in a trade-off of image noise in our study. Indeed, in our obese study population, similar image noise was detected for a standard-definition protocol compared with the high definition/ASIR protocol, while, at the same time, higher vessel attenuation and visibility of details were achieved in the high-defintion protocol. ASIR allows reduction of pixel variance that is statistically unlikely to represent anatomic structures without trade-off in spatial resolution. Thus, reconstructions with ASIR yield images with reduced noise and a more homogenous appearance that differs from those obtained with traditional FBP as the borders are smoothed while the central area of the lesion appears more dense [9, 23]. This may result in a higher attenuation level of iodinated contrast media and an increase in vessel signal intensity as observed in the present study.

Our study has several limitations, which have to be considered. First, the present study does not represent a head-to-head comparison, as two different patient groups had to be identified because repeat scanning of the same patients would not be appropriate due to radiation exposure and ethical issues. However, patients were specifically matched on a case–control basis for age, gender, BMI and calcifications to ensure a fair comparison between techniques. Second, individual hemodynamic differences may have influenced our study results, even though the bolus tracking method was used in all subjects in order to optimize contrast-agent injection. The most important limitation of this study is the absence of comparison to the "gold standard" of invasive angiography in most patients. Thus, we were not able to evaluate whether ASIR images would improve accuracy in the detection of CAD. Future studies with a focus on direct comparison between HDCT scanning and invasive angiography in this patient group will be required.

In summary, our findings suggest that the use of a novel CT scanner with 0.23-mm spatial resolution improves overall image quality and coronary artery visualization in overweight and obese patients compared with SDCT scanning with 0.625-mm spatial resolution, without increasing radiation dose. Due to the additional use of ASIR in HDCT, these improvements in spatial resolution and visualization did not occur at the expense of increased image noise, as opposed to the use of high resolution or sharp convolution kernels in HDCT scanning. In conclusion, the use of ASIR protocols in combination with HDCT does efficiently work to improve image quality in overweight and obese patients.

Acknowledgments The study was supported by grants from the Swiss National Science Foundation (SNSF) to P.A.K., C.G. and to M.F.

Ethical standard All procedures followed were in accordance with the ethical standards of the responsible committee on human experimentation (institutional and national) and with the Helsinki Declaration of 1975, as revised in 2008. The need for written informed consent in this study was waived by the institutional review board (local ethics committee) since, according to Swiss law on clinical investigations, informed consent is not required if the nature of the study is purely retrospective.

Conflict of interest The authors declare that they have no conflict of interest.

References

1. Romero-Corral A, Montori VM, Somers VK, Korinek J, Thomas RJ, Allison TG et al (2006) Association of bodyweight with total mortality and with cardiovascular events in coronary artery disease: a systematic review of cohort studies. Lancet 368(9536):666–678
2. Yoshimura N, Sabir A, Kubo T, Lin PJ, Clouse ME, Hatabu H (2006) Correlation between image noise and body weight in coronary CTA with 16-row MDCT. Acad Radiol 13(3):324–328
3. Raff GL, Gallagher MJ, O'Neill WW, Goldstein JA (2005) Diagnostic accuracy of noninvasive coronary angiography using 64-slice spiral computed tomography. J Am Coll Cardiol 46(3):552–557
4. Chinnaiyan KM, McCullough PA, Flohr TG, Wegner JH, Raff GL (2009) Improved noninvasive coronary angiography in morbidly obese patients with dual-source computed tomography. J Cardiovasc Comput Tomog. 3(1):35–42
5. Silva AC, Lawder HJ, Hara A, Kujak J, Pavlicek W (2010) Innovations in CT dose reduction strategy: application of the

adaptive statistical iterative reconstruction algorithm. AJR Am J Roentgenol 194(1):191–199
6. Leipsic J, Heilbron BG, Hague C (2012) Iterative reconstruction for coronary CT angiography: finding its way. Int J Cardiovasc Imaging 28(3):613–620
7. Leipsic J, Labounty TM, Heilbron B, Min JK, Mancini GB, Lin FY et al (2010) Estimated radiation dose reduction using adaptive statistical iterative reconstruction in coronary CT angiography: the ERASIR study. AJR Am J Roentgenol 195(3):655–660
8. Pontone G, Andreini D, Bartorelli AL, Bertella E, Mushtaq S, Foti C et al (2012) Feasibility and diagnostic accuracy of a low radiation exposure protocol for prospective ECG-triggering coronary MDCT angiography. Clin Radiol 67(3):207–215
9. Leipsic J, Labounty TM, Heilbron B, Min JK, Mancini GB, Lin FY et al (2010) Adaptive statistical iterative reconstruction: assessment of image noise and image quality in coronary CT angiography. AJR Am J Roentgenol 195(3):649–654
10. Kazakauskaite E, Husmann L, Stehli J, Fuchs T, Fiechter M, Klaeser B et al (2013) Image quality in low-dose coronary computed tomography angiography with a new high-definition CT scanner. Int J Cardiovasc Imaging 29(2):471–477
11. Desai GS, Uppot RN, Yu EW, Kambadakone AR, Sahani DV (2012) Impact of iterative reconstruction on image quality and radiation dose in multidetector CT of large body size adults. Eur Radiol 22(8):1631–1640
12. Ghadri JR, Kuest SM, Goetti R, Fiechter M, Pazhenkottil AP, Nkoulou RN et al (2011) Image quality and radiation dose comparison of prospectively triggered low-dose CCTA: 128-slice dual-source high-pitch spiral versus 64-slice single-source sequential acquisition. Int J Cardiovasc Imaging 28(5): 1217–1225
13. Buechel RR, Husmann L, Herzog BA, Pazhenkottil AP, Nkoulou R, Ghadri JR et al (2011) Low-dose computed tomography coronary angiography with prospective electrocardiogram triggering: feasibility in a large population. J Am Coll Cardiol 57(3): 332–336
14. Husmann L, Herzog BA, Gaemperli O, Tatsugami F, Burkhard N, Valenta I et al (2009) Diagnostic accuracy of computed tomography coronary angiography and evaluation of stress-only single-photon emission computed tomography/computed tomography hybrid imaging: comparison of prospective electrocardiogram-triggering vs. retrospective gating. Eur Heart J 30(5):600–607
15. Herzog BA, Husmann L, Burkhard N, Valenta I, Gaemperli O, Tatsugami F et al (2009) Low-dose CT coronary angiography using prospective ECG-triggering: impact of mean heart rate and heart rate variability on image quality. Acad Radiol 16(1):15–21
16. Raff GL, Goldstein JA (2007) Coronary angiography by computed tomography: coronary imaging evolves. J Am Coll Cardiol 49(18):1830–1833
17. McNulty PH, Ettinger SM, Field JM, Gilchrist IC, Kozak M, Chambers CE et al (2002) Cardiac catheterization in morbidly obese patients. Catheter Cardiovasc Interv 56(2):174–177
18. Leschka S, Stinn B, Schmid F, Schultes B, Thurnheer M, Baumueller S et al (2009) Dual source CT coronary angiography in severely obese patients: trading off temporal resolution and image noise. Invest Radiol 44(11):720–727
19. Kropil P, Rojas CA, Ghoshhajra B, Lanzman RS, Miese FR, Scherer A et al (2012) Prospectively ECG-triggered high-pitch spiral acquisition for cardiac CT angiography in routine clinical practice: initial results. J Thorac Imaging 27(3):194–201
20. Srichai MB, Lim RP, Donnino R, Mannelli L, Hiralal R, Avery R et al (2012) Low-dose, prospective triggered high-pitch spiral coronary computed tomography angiography: comparison with retrospective spiral technique. Acad Radiol 19(5):554–561
21. Paul NS, Kashani H, Odedra D, Ursani A, Ray C, Rogalla P (2011) The influence of chest wall tissue composition in determining image noise during cardiac CT. AJR Am J Roentgenol 197(6):1328–1334
22. Xu L, Zhang Z (2010) Coronary CT angiography with low radiation dose. Int J Cardiovasc Imaging 26(Suppl 1):17–25
23. Gebhard C, Fiechter M, Fuchs TA, Ghadri JR, Herzog BA, Kuhn F et al (2012) Coronary artery calcium scoring: influence of adaptive statistical iterative reconstruction using 64-MDCT. Int J Cardiol. doi:10.1016/j.ijcard.2012.08.003